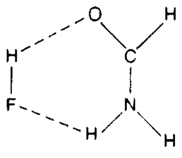

3

Conclusions

Hydrogen-bonded amide–HF complexes have been produced in solid argon and characterized by FTIR spectroscopy. The complexes are proposed to have cyclic structures involving two hydrogen bonds. The primary hydrogen bond at the carbonyl oxygen is affected by the nature of the R substituent; the more electron-donating R group displaces ν_s(HF) to lower frequencies. From the measurements of ν_s encountered in these experiments, the hydrogen bond strength is comparable to that of amine–HF complexes. The secondary hydrogen bond between amido hydrogen and the fluorine atom is characterized by blue-shifting on hydrogen motions of the NH_2 group, especially $\tau(NH_2)$.

The infrared spectroscopic evidence for hydrogen bonding of HF at the oxygen–amide site is based on comparison with shifts in base submolecule modes for acetone, acetic acid, ammonia, and methylamine complexes with HF. Shifts in skeletal stretching vibrations parallel the behavior for carbonyl complexes and shifts in $-NH_2$ bending and C–N stretching vibrations oppose trends in amine complexes. In particular, the HF/DF shift observed for the carbonyl stretching modes in the amide–acid complexes verifies the strong coupling between these bond stretching modes and requires acid binding to the carbonyl oxygen site. Base submolecule modes are sensitive to the site of attachment of the acid, and shifts in the spectrum of the complex provide qualitative structural information on the complicated but important amide–acid complexes.

Acknowledgment. We thank W. J. Pitts for sample purification and synthesis of d_2-A, R. B. Martin for helpful discussions on amide protonation, and NSF for financial support through grant CHE85-16611.

Registry No. CH_3CONH_2, 60-35-5; $HCONH_2$, 75-12-7; CF_3CONH_2, 354-38-1; $CH_3CON(CH_3)_2$, 127-19-5; HF, 7664-39-3; D_2, 7782-39-0.

Assignment of the Charge-Transfer Excited States of Bis(N-heterocyclic) Complexes of Copper(I)

W. L. Parker and G. A. Crosby*

Chemical Physics Program, Washington State University, Pullman, Washington 99164-4620

(Received: January 3, 1989)

Four title complexes were investigated spectroscopically to ascertain the natures of their singlet and triplet excited-state manifolds. Absorption (room temperature, RT) and luminescence (77 K) spectra were measured for all the species. Augmented by additional measurements for the bis(2,9-dimethyl-4,7-diphenyl-1,10-phenanthroline)copper(I) ion [MCD (RT), excitation polarization measurements (100 K), and variations of both the emission spectra and the lifetimes as a function of temperature], group theoretical assignments of both the low-lying singlet and triplet charge-transfer states have been made. The model invokes a lowering of the symmetry from D_{2d} to D_2 to account for the experimental observations.

Introduction

Charge-transfer (CT) excited states of metal complexes are provoking intense study, particularly within the context of attempts to design efficient solar energy conversion processes. Since several classes of molecules containing the copper(I) ion have been observed to emit light in fluid solution,[1-3] attention has begun to focus on these substances. Although excitation of CT excited states has been shown to induce electron-transfer reactons,[4,5] complete group theoretic assignments of the nature of the electronic states responsible for the visible absorption and emission spectra have not yet appeared. In this study we focus on the rigid matrix spectra of $[Cu(NN)_2]^+$ species (NN = substituted 2,2′-bipyridine or substituted 1,10-phenanthroline) and propose a group theoretical model to rationalize the results of extensive photophysical measurements on these interesting substances.

Experimental Section

Preparation of Materials. All the complexes were synthesized according to the scheme of Schilt and Taylor,[6] which starts with copper sulfate as the primary salt and employs hydroxylamine hydrochloride to reduce the metal. Addition of the desired ligand (Aldrich Chemical Co.) produced the crude product, which precipitated slowly as the perchlorate salt after the addition of $NaClO_4$ to the boiling aqueous solution. Satisfactory elemental analyses were obtained in all cases. The complexes formed well-defined crystals and were stable in air, both in the solid state and in the solvents used for the spectroscopic measurements. The following $[Cu(NN)_2]ClO_4$ compounds were prepared in the described manner: $[Cu(bpy)_2]ClO_4$; $[Cu(dmb)_2]ClO_4$; $[Cu(phen)_2]ClO_4$; $[Cu(bcn)_2]ClO_4$, where bpy = 2,2′-bipyridine, dmb = 6,6′-dimethyl-2,2′-bipyridine, phen = 1,10-phenanthroline, bcn = 2,9-dimethyl-4,7-diphenyl-1,10-phenanthroline (bathocuproine).

Sample Preparation. All spectroscopic measurements were performed in ethanol/methanol solutions at room temperature (absorption and MCD), at 77 K (absorption and emission), or at 100 K (polarization ratio measurements). Methanol was J.

---

(1) Kirchhoff, J. R.; Gamache, R. E., Jr.; Blaskie, M. W.; Del Paggio, A. A.; Lengel, R. K.; McMillin, D. R. *Inorg. Chem.* **1983**, *22*, 2380.

(2) Dietrich-Buchecker, C. O.; Marnot, P. A.; Sauvage, J. P.; Kirchhoff, J. R.; McMillin, D. R. *J. Chem. Soc., Chem. Commun.* **1983**, 513.

(3) Radar, R. A.; McMillin, D. R.; Buckner, M. T.; Matthews, T. G.; Casadonte, D. J.; Lengel, R. K.; Whittaker, S. B.; Darmon, L. M.; Lytle, F. E. *J. Am. Chem. Soc.* **1981**, *103*, 5906.

(4) McMillin, D. R.; Buckner, M. T.; Ahn, B. T. *Inorg. Chem.* **1977**, *16*, 943.

(5) Ahn, B. T.; McMillin, D. R. *Inorg. Chem.* **1981**, *20*, 1427.

(6) Schilt, A. A.; Taylor, R. C. *J. Inorg. Nucl. Chem.* **1959**, *9*, 211.

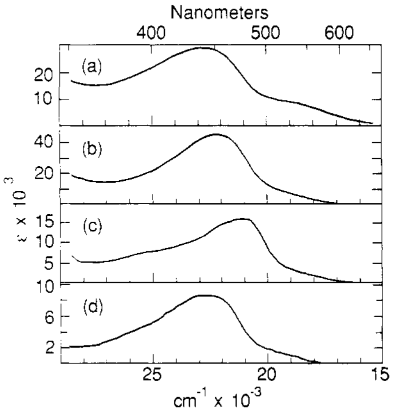

Figure 1. Effect of ligand modification on the visible absorption spectra of some cuprous complexes in 4:1 ethanol/methanol at room temperature: (a) $[Cu(bpy)_2]ClO_4$; (b) $[Cu(dmb)_2]ClO_4$; (c) $[Cu(bcn)_2]ClO_4$; (d) $[Cu(phen)_2]ClO_4$.

T. Baker Photrex grade and was used without further purification. Ethanol was distilled over the corresponding Grignard reagent through a Vigreau column.

Lifetimes (300–4.2 K) were measured for $[Cu(bcn)_2]ClO_4$ dissolved in a poly(methyl methacrylate) (PMM) plastic. The methacrylate monomer was distilled from activated charcoal under vacuum. After the complex had been dissolved in the liquid monomer, azobis(isobutyronitrile) was added as a polymerization initiator and the samples were cast in 2-oz glass vials and incubated for 3 days. The PMM rods produced in this manner were then machined and polished before they were mounted onto the Dewar block.

Spectroscopic Measurements. Absorption spectra were recorded on a Cary Model 14 or on a Hitachi Perkin-Elmer Model 330 UV–vis–near-IR spectrophotometer. Data were collected digitally and transferred to a PDP 11/34 or a PDP 11/2 computer, respectively.

The lifetime vs temperature of the luminescence of $[Cu(bcn)_2]ClO_4$ in PMM was recorded by monitoring the total emission, filtered through a $NaNO_2$ cell, with a RCA 7102 photomultiplier tube, which had been wired for pulsed operation. The data were collected on a Biomation 6500 waveform recorder and then stored and processed by the PDP 11/2 computer. Excitation and emission polarization ratio spectra were measured with an apparatus similar to that used by Agnew et al.[7] constructed according to the design suggested by Hipps and Crosby.[8] The sensitivity of the apparatus was greatly enhanced by the use of all ac detection. The excitation was chopped at 100 Hz, making the detection of the total emission an ac measurement rather than the dc measurement used previously. This method reduced complications from stray light substantially and allowed the use of narrower slits. This improvement also permitted a simpler, slightly off-axis, 180° optical alignment without interference from the excitation source. A PAR JB-4 lock-in amplifier was used to lock in on the 100-Hz component of the signal, and a PAR Model 113 differential preamplifier was used to increase the input impedance of the lock-in amplifier. In spite of the improved sensitivity obtained with these electronics, the light levels were so low that only the polarization ratio measurements, $P = (I_{\parallel} - I_{\perp})/(I_{\parallel} + I_{\perp})$, for $[Cu(bcn)_2]ClO_4$ could be reliably recorded. The polarization ratio experiment mandates that the sample exist in a strain-free rigid medium, which was only attainable for these systems in an ethanol/methanol glass that formed near the temperature of 100 K. The light level problem was exacerbated by the fact that the intensity of the emission decreased rapidly below 150 K.

MCD spectra were obtained by employing the same signal processing electronics as those used for the polarization ratio measurements. A 4.7-T magnetic field was generated at the sample by an Oxford Instruments Spectromag II superconducting solenoid, outfitted with a room temperature bore. To record MCD spectra the lock-in amplifier was tuned to 50 kHz and not to 100 kHz as required for the polarization ratio measurement.[8]

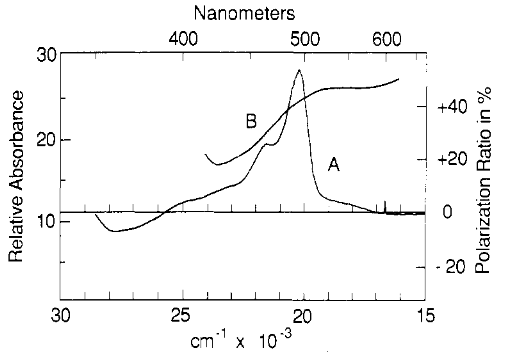

Figure 2. Absorption and polarization spectra of $[Cu(bcn)_2]ClO_4$ in 4:1 ethanol/methanol glass: A, absorption at 77 K; B, excitation polarization ratio at 100 K monitored at 750 nm.

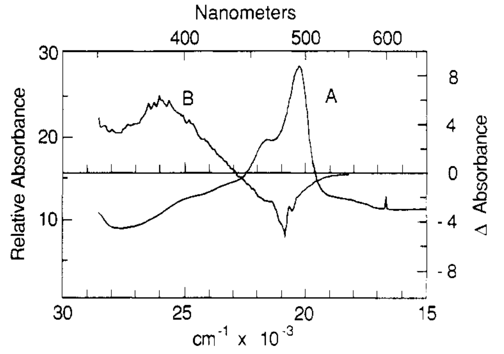

Figure 3. Spectra of $[Cu(bcn)_2]ClO_4$ in 4:1 ethanol/methanol: A, absorption at 77 K; B, magnetic circular dichroism at room temperature.

Results

Absorption, Polarization, and MCD Results. In Figure 1 we present the visible absorption spectra of a series of related cuprous complexes. Since the metal ion has a $(3d)^{10}$ configuration, one expects pseudotetrahedral geometry. As expected from their chemical similarity, the complexes possess similar spectra. In each case the visible region is dominated by a broad transition maximizing in the range of 440–480 nm. The broad peak shifts red when phenyl groups are introduced to the phenanthroline backbone as is evidenced from the comparison of the phen and bcn complexes. The phenyl groups also serve to increase considerably the intensity of the observed band. Substituent effects have been noted before.[2] Closer inspection reveals other pertinent differences among the spectra. Particularly important to us (vide infra) is the broad diffuse shoulder extending to longer wavelengths that is obvious in all the curves. Moreover, this shoulder is most prominent in the $[Cu(bpy)_2]^+$ species, which is not sterically hindered, and least prominent in those species that have methyl substituents in the "steric" positions (6,6′ in bpy; 2,9 in phen). Substituents in these positions hinder rotation of the ligands.

Figure 2 shows the absorption spectrum of $[Cu(bcn)_2]ClO_4$ in an organic glass at 77 K. Superimposed on this spectrum is the plot of the excitation polarization ratio P, measured as a function of wavelength with respect to the emission monitored near its band maximum (ca. 750 nm). The polarization ratio was recorded at 100 K. Due to the low intensity of emission at 100 K, the signal had considerable noise, but the result is unmistakable. The main absorption band, the high-energy shoulder, and the *diffuse shoulder at lower energy* are all strongly polarized in the same direction. From the magnitude of P (0.40) we conclude that both the absorption and emission bands are z polarized (at 100 K).[9]

---

(7) Agnew, S. F.; Stone, M. L.; Crosby, G. A. *Chem. Phys. Lett.* **1982**, *85*, 57.

(8) Hipps, K. W.; Crosby, G. A. *J. Phys. Chem.* **1979**, *83*, 555.

(9) Parker, W. L.; Crosby, G. A. *Chem. Phys. Lett.* **1984**, *105*, 544.

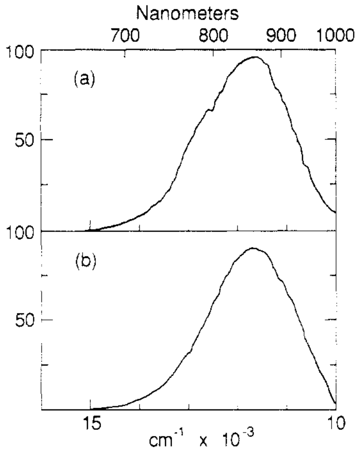

Figure 4. Emission spectra of (a) $[Cu(bcn)_2]ClO_4$ and (b) $[Cu(2,9\text{-dimethyl-phen})_2]ClO_4$ in CH_2Cl_2 at room temperature.

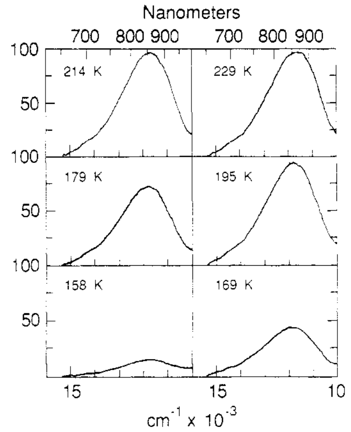

Figure 5. Intensity variation with temperature of the emission spectrum of $[Cu(bcn)_2]ClO_4$. Sample matrix was poly(methyl methacrylate). All spectra were normalized to the emission at 229 K.

In Figure 3 we reproduce the room temperature MCD spectrum along with the 77 K absorption spectrum of $[Cu(bcn)_2]ClO_4$. Comparison of this figure with the preceding one shows that the MCD is changing sign in the range where the polarization ratio is also undergoing a sign inversion. We interpret these results to signify that the MCD curve is not the result of a genuine A term but is the superposition of B terms of opposite sign arising from two or more transitions. Thus both the polarization ratio and the MCD results point to a visible absorption spectrum dominated at low energy by transitions to states that are allowed in z polarization. Our interpretation of the MCD results is not in accord with the work of Hollebone et al., who interpreted the MCD as a pure A term arising from a degenerate (E) state.[10]

Emission Results. As a rule, for bis complexes of the N-heterocycles only those that contain substituents in the "steric" positions emit light at all, irrespective of the temperature of the medium. Bands of the two strongest emitters in fluid CH_2Cl_2 are presented in Figure 4. Both display a broad luminescence peaking at ca. 860 nm with a perceptible shoulder on the high-energy side. The shoulder is particularly evident in the spectrum of $[Cu(bcn)_2]ClO_4$. When held in a PMM matrix, the emission intensity decreases monotonically with decreasing temperatures and a red shift of about 1000 cm^{-1} occurs. This is demonstrated for $[Cu(bcn)_2]ClO_4$ in Figure 5. The result is to be compared with that of Kirchhoff et al.,[1] who reported a peak shift of about 1800 cm^{-1} with time for the emission in fluid solution determined from time-resolved spectral measurements. For $[Cu(bcn)_2]ClO_4$ the measured lifetime increases monotonically from ca. 525 ns at room temperature to ca. 780 ns at 4.2 K in PMM (Figure 6). The magnitude of the decay time and the lack of any overlap of the emission spectrum with the absorption spectrum indicate strongly that the luminescence is indeed a phosphorescence. The temperature variation of τ_m and the shift of emission maximum suggest that at least two states separated by $\sim 10^3$ cm^{-1} are involved.

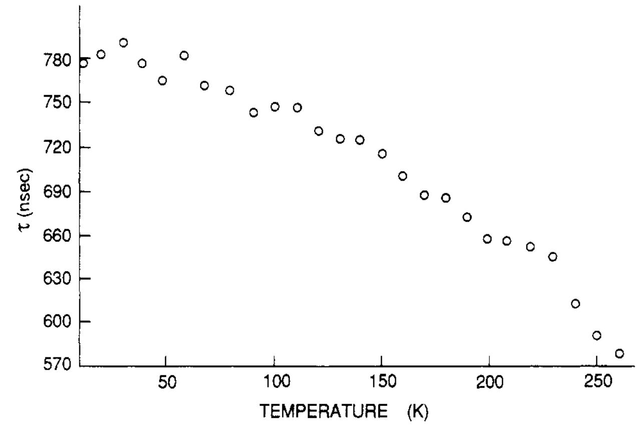

Figure 6. Variation of the measured lifetime of $[Cu(bcn)_2]ClO_4$ with temperature. All logarithmic plots of luminescence decay were somewhat nonlinear.

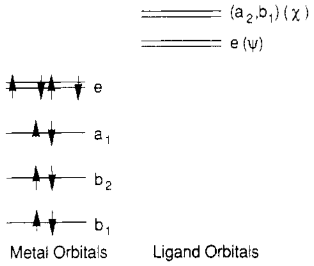

Figure 7. Proposed orbital scheme for $[Cu(NN)_2]^+$ ions in D_{2d} symmetry. The Ψ and χ labels refer to individual ligand orbitals that are antisymmetric (Ψ) and symmetric (χ) with respect to the principal C_2 axis of the complex. These form the basis for the indicated representations in D_{2d}.

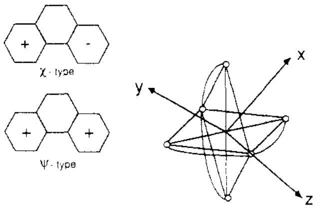

Figure 8. Symmetrized coordinate system chosen for a complex in D_{2d} symmetry with illustrations of the molecular orbital designations used for the ligands.

Molecular Geometry

Previous assignments[11-13] of the absorption spectra of bis(N-heterocyclic) complexes of copper(I) have always been based on D_{2d} microsymmetry about the metal ion, but recent X-ray crystallographic data provide a different perspective on this problem. The X-ray structures of $[Cu(dmb)_2]BF_4$[14] and $[Cu(2,9\text{-dimethyl-phen})_2]NO_3$[15] both indicate that the cation microsymmetry is not D_{2d}. In each case the angle between ligand planes is closer to 80° rather than the required 90° value. Other deviations from D_{2d} include inequivalence of the ligands and even unequal nitrogen–metal bond distances for the same ligand. These latter distortions are small, however, and we prefer to discuss these cuprous complexes in terms of ideal D_{2d} symmetry distorted to D_2 by a simple rotation of the planes of the two N-heterocyclic

---

[10] Hollebone, B. R.; Mason, S. F.; Thomson, A. J. *Symp. Faraday Soc.* **1969**, No. 3, 146.

[11] Day, P.; Sanders, N. *J. Chem. Soc. A* **1967**, 1530.

[12] Day, P.; Sanders, N. *J. Chem. Soc. A* **1967**, 1536.

[13] Irving, H.; Williams, R. J. P. *J. Chem. Soc.* **1953**, 3192.

[14] Burke, P. J.; McMillin, D. R.; Robinson, W. R. *Inorg. Chem.* **1980**, *19*, 1211.

[15] Hamalainen, R.; Ahlgren, M.; Terpeinen, U.; Raikas, T. *Cryst. Struct. Commun.* **1979**, *8*, 75.

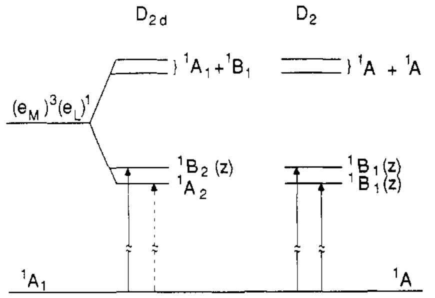

Figure 9. Proposed singlet energy level scheme for $[Cu(NN)_2]^+$ complexes: → allowed transition; ---→ forbidden transition.

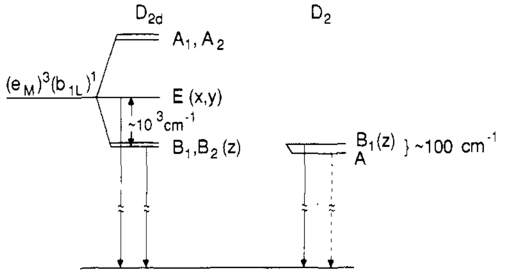

Figure 10. Proposed triplet energy level scheme for $[Cu(NN)_2]^+$ complexes. Energy separations are taken from experimental results. → allowed transition; ---→ forbidden transition.

ligands away from orthogonality.

Orbital Model

Orbital Sequences. In D_{2d} symmetry we assume the scheme given in Figure 7 for the metal d orbitals and the lowest lying unoccupied π orbitals of the N-heterocyclic ligand system. Placing the metal e orbital highest is in accord with crystal field[16] extended Hückel and MS SCF-Xα calculations.[17]

To select the lowest lying empty ligand orbitals we appeal to simple HMO theory. A planar symmetric (phen or bpy) bidentate ligand possesses C_{2v} symmetry. Molecular orbitals of the π type may be simply subdivided into two sets,[18] those which are symmetric about the principal C_2 axis, χ-type, and those which are antisymmetric with respect to this axis, ψ-type. These are depicted schematically in Figure 8 for 1,10-phenanthroline.

For bis complexes possessing D_{2d} symmetry the geometry and axis system is shown in Figure 8. The ligand C_2 axis is preserved in the complex. The pairs of ψ-type orbitals form a basis for the e irreducible representation, whereas the χ-type set breaks into a (a_2,b_1) pair in D_{2d}. Simple HMO theory of the free ligands places the orbitals in the order given in the diagram, and we retain this ordering in the complex. Our experimental results also point to this ordering (vide infra). In the ground state of the molecule the 3d shell of the metal atom is complete.

Proposed Singlet State Manifold. The visible absorption bands are clearly charge transfer in nature. They are intense, shift substantially with change of ligand substituents, and accompany a metal in a low, but easily oxidizable, oxidation state. Thus they satisfy the generally accepted criteria for charge-transfer-to-ligand (CTTL) transitions.[19] A simple one-electron promotion from e(metal) to e(ligand) leads to the diagram given in Figure 9 for singlet states.

As depicted in Figure 9 the direct product $(e_M \otimes e_L)$ yields $A_1 \oplus A_2 \oplus B_1 \oplus B_2(z)$ in D_{2d} and only the $^1B_2(z)$ is formally allowed. First-order electrostatic terms will split this configuration into four nondegenerate states. In the diagram we have placed the $^1B_2$ state second in energy and we correlate it with the strong z-allowed absorption peak dominant in all the spectra. Our reasons for placing the $^1A_2$ state lowest is implicit in the second column in the figure. Lowering the symmetry to D_2 confers allowed character to the previously forbidden $^1A_2$ level, which becomes allowed with z polarization. As the symmetry is lowered (by rotation of the ligands about the C_2 axis), the $^1A_2$ intensity is expected to increase with the degree of distortion away from D_{2d}. We assign this state to the low-energy shoulder that appears in the absorption spectra of all the molecules, but which is especially prominent in the $[Cu(bpy)_2]^+$ spectrum. This latter molecule is precisely the one expected to deviate most from D_{2d} geometry. For those species containing methyl groups in the positions that will hinder rotation, less intensity is expected, and this is what is observed (Figure 1).

The electronic model accounts for both the dominant absorption peak and the low-energy shoulder. The high-energy shoulder (ca. 460 nm in Figures 2 and 3) has been assigned to a vibrational satellite in analogous complexes on the basis of evidence from infrared and resonance Raman spectra.[17] We agree with the previous vibrational assignment since the polarization ratio remains constant over this peak.

Proposed Triplet-State Manifold. The ca. 10^3-cm^{-1} red shift of the band maximum of the luminescence of $[Cu(bcn)_2]ClO_4$, the dramatic decrease in intensity as the temperature is lowered to 100 K, and the increase in measured lifetime as the temperature is lowered clearly signal the emanation of radiation from more than one electronic state. Moreover, at ca. 100 K the phosphorescence is predominately z polarized. Thus, we look for a triplet term that will give us ca. 10^3-cm^{-1} splitting with at least two allowed components. We begin by restricting the arguments to D_{2d} symmetry. In D_{2d} the $S = 1$ spin representation breaks into $A_2 + E$. Of the orbitally nondegenerate states only $^3B_1$ yields two formally allowed components $[E(x,y) + B_2(z)]$ and these are expected to be split by spin–orbit coupling only in second order. The temperature dependence of the intensity indicates, however, a splitting of ca. 10^3 cm^{-1}, far too large to be only second order in spin–orbit coupling. Thus we conclude that no simple *nondegenerate* triplet term can be responsible for the observed behavior of the phosphorescence. This eliminates assignment of the lowest triplet state to the $(e_M)(\psi)$ configuration. In D_{2d}, however, a ^3E term spans the entire set of irreducible representations. In fact, a simple spin–orbit coupling calculation predicts that a ^3E term, which could result from a $(e_M)(\chi)$ configuration, should split into three levels as shown in Figure 10, with a splitting that is first order in the spin–orbit coupling constant of the metal ion (see Appendix). Two of the sets of levels are accidentally degenerate to first order, but the middle level (E) is strictly degenerate in D_{2d}. The order of the levels depends on the nature of the excited configuration assumed but the magnitude of the splitting is fixed. Four our system we assume the arrangement given in Figure 10 in order to conform with the observation that the luminescence is z polarized at 100 K, a temperature insufficient, as determined by the calculation, to populate the $E(x,y)$ level.

Although our assignment of the emitting states is not definitive, the energy-level scheme in Figure 10 is appealing for other reasons. If the symmetry is lowered to D_2, then the (B_1,B_2) pair correlates to A and $B_1(z)$, respectively. The A state is forbidden. Thus, as the temperature is lowered from 100 K, the phosphorescence is expected to remain z polarized, but to decrease in intensity as the very lowest state (A in D_2) becomes preferentially populated. Since the intensity decrease occurs at ca. 150 K, we estimate this $(A-B_1)$ splitting to be about 100 cm^{-1}. The magnitude of the splitting would depend both on second-order spin-orbit coupling and the amount of distortion away from D_{2d}.

If Figure 10 is indeed a faithful representation of the lowest emitting levels in the molecules, then one expects the polarization to switch from z to x,y as the temperature is raised. All attempts to verify this prediction have failed because of our inability to identify a suitable strain-free rigid matrix at temperatures far from 100 K in either direction.

Structural Spectroscopic Correlations

The model that we propose for the excited-state manifold in these $[Cu(NN)_2]^+$ ions rests firmly on the assignment of the

---

(16) Solomon, E. I.; Hare, J. W.; Dooley, D. M.; Dawson, J. H.; Stephens, P. J.; Gray, H. B. *J. Am. Chem. Soc.* **1980**, *102*, 168.

(17) Daul, C.; Schläpfer, C. W.; Goursot, A.; Penigault, E.; Weber, J. *Chem. Phys. Lett.* **1981**, *78*, 304.

(18) Orgel, L. E. *J. Chem. Soc.* **1961**, 3683.

(19) Crosby, G. A. *Acc. Chem. Res.* **1975**, *8*, 231.

principal absorption maximum in all these molecules to a z-polarized transition of $B_2(D_{2d})$ symmetry. This assignment implies that electronic charge is transferred to the NN ligands along the principal axis of the complex during the transition. This is intuitively appealing for CTTL transitions. The incidence of the low-lying $(e_M)(e_L)$ configuration also points toward considerable "back-bonding" in the molecules since this configuration possesses a A_1 component that can mix with the A_1 ground state (vide supra). Indeed the mixing of this CTTL configuration into the ground state can be related to the intensity of the CTTL transition $[{}^1A_1 \rightarrow {}^1B_2(z)]$ by an extension of the ideas of Mulliken[20] for CT transition dipole strength in simple organic donor–acceptor complexes to metal complexes possessing high symmetry. A quantitative development of these ideas will be published elsewhere.[21] Finally, we wish to emphasize that the distortion of the complexes away from D_{2d} symmetry can be viewed as a manifestation of CT configurational mixing with the ground state. Viewed chemically, adding a CTTL component to the ground-state wave function confers $[\mathrm{Cu(II)}[(\mathrm{NN})_2^-]]^+$ character to the latter. Since copper(II) is known to prefer square planar geometry, this admixture would be expected to lead to a distortion away from D_{2d} toward D_{2h}. The degree of rotation of the ligands would be controlled both by the electronic (mixing) and steric factors. This same argument can be applied to the CTTL excited-state manifolds and accounts for the lack of emission from $[\mathrm{Cu(NN)_2}]^+$ species that can rotate in the excited state and thus further stabilize the forbidden lowest excited electronic state (A) from which dipole transitions to the ground state are forbidden.

Acknowledgment. This work was supported in part by the Office of Naval Research and the National Science Foundation under Grants No. CHE-8119060 and CHE-8421282.

Appendix

Spin–Orbit Coupling of a ³E Charge-Transfer Term in D_{2d} Symmetry. The spin–orbit coupling Hamiltonian is frequently written as

$$\mathbf{H}_{\mathrm{SO}} = \sum_i \xi_i(r) l_i \cdot s_i$$

In the Russell–Saunders coupling limit this is replaced by

$$\mathbf{H}_{\mathrm{so}} = \lambda \mathbf{L} \cdot \mathbf{S} \qquad \text{where } \mathbf{L} = \sum_i l_i \text{ and } \mathbf{S} = \sum_i s_i$$

which leads to the Landé interval rule famous from atomic spectroscopy. In order to use the irreducible tensor method in our calculation we must express the spin–orbit coupling operator in irreducible form. Silver[22] expresses the spin–orbit coupling operator in the Russell–Saunders limit as

$$\mathbf{H}_{\mathrm{so}} = \lambda(S_+L_- + S_-L_+ - iL_zS_0)$$

In first-order perturbation theory only the last element will contribute within the ³E term. The triplet spin functions span the E and A_2 irreducible representations of the D_{2d} point group, with the $m_s = 0$ portion of the spin function transforming as the A_2 irreducible representation. The ³E term is 6-fold degenerate. The final symmetries spanned by the ³E term in the D_{2d} point group are

$${}^3\mathrm{E}\begin{cases} \mathrm{e(spin)} \otimes \mathrm{e(space)} \in \{\mathrm{A_1} \oplus \mathrm{A_2} \oplus \mathrm{B_1} \oplus \mathrm{B_2}\} \\ \mathrm{a_2(spin)} \otimes \mathrm{e(space)} \in \mathrm{E} \end{cases}$$

Because $m_s = 0$ in the state of final symmetry E, it is obvious that the matrix element $\langle \mathrm{E}|iL_zS_0|\mathrm{E}\rangle$ is zero, and we need only evaluate the matrix elements

$$\langle \mathrm{A_1}|L_zS_0|\mathrm{A_1}\rangle, \quad \langle \mathrm{A_2}|L_zS_0|\mathrm{A_2}\rangle, \quad \langle \mathrm{B_1}|L_zS_0|\mathrm{B_1}\rangle, \quad \langle \mathrm{B_2}|L_zS_0|\mathrm{B_2}\rangle$$

We facilitate this task by uncoupling the functions into spatial and spin parts

$$|\Gamma m_\Gamma\rangle = \sum_{A,B,\alpha,\beta} \langle A\alpha B\beta|\Gamma m_\Gamma\rangle |A\alpha B\beta\rangle$$

We can use the V coefficients defined by Griffith[23]

$$V\begin{pmatrix} A & B & \Gamma \\ -\alpha & -\beta & m_\Gamma \end{pmatrix} = \lambda(\Gamma)^{-1/2}\langle A\alpha B\beta|\Gamma m_\Gamma\rangle$$

Recognizing that the point group D_{2d} is isomorphic with D_4 we may use the complex V coefficients from Griffith's Appendix D, Table D.3.2. We find

$$|\mathrm{A_1}\rangle = \frac{1}{2^{1/2}}\{|\mathrm{E} - \mathrm{E}+\rangle + |\mathrm{E} + \mathrm{E}-\rangle\}$$

$$|\mathrm{A_2}\rangle = \frac{i}{2^{1/2}}\{-|\mathrm{E} - \mathrm{E}+\rangle + |\mathrm{E} + \mathrm{E}-\rangle\}$$

$$|\mathrm{B_1}\rangle = \frac{1}{2^{1/2}}\{|\mathrm{E} + \mathrm{E}+\rangle + |\mathrm{E} - \mathrm{E}-\rangle\}$$

$$|\mathrm{B_2}\rangle = \frac{i}{2^{1/2}}\{|\mathrm{E} + \mathrm{E}+\rangle - |\mathrm{E} - \mathrm{E}-\rangle\}$$

and

$$\begin{aligned}\langle \mathrm{A_1}|L_zS_0|\mathrm{A_1}\rangle &= \\ &\frac{1}{2}\{\langle \mathrm{E} + \mathrm{E} - |L_zS_0|\mathrm{E} + \mathrm{E} -\rangle + \langle \mathrm{E} + \mathrm{E} - |L_zS_0|\mathrm{E} - \mathrm{E}+\rangle\} = \\ &\frac{1}{2}\langle \mathrm{E}\|L\|\mathrm{E}\rangle\langle \mathrm{E}\|S\|\mathrm{E}\rangle\left\{V\begin{pmatrix} \mathrm{E} & \mathrm{A_1} & \mathrm{E} \\ - & \mathrm{a_1} & + \end{pmatrix}V\begin{pmatrix} \mathrm{E} & \mathrm{A_1} & \mathrm{E} \\ + & \mathrm{a_1} & - \end{pmatrix} + \right. \\ &\left. V\begin{pmatrix} \mathrm{E} & \mathrm{A_1} & \mathrm{E} \\ + & \mathrm{a_1} & - \end{pmatrix}V\begin{pmatrix} \mathrm{E} & \mathrm{A_1} & \mathrm{E} \\ - & \mathrm{a_1} & + \end{pmatrix}\right\} = \frac{1}{2}\langle \mathrm{E}\|L\|\mathrm{E}\rangle\langle \mathrm{E}\|S\|\mathrm{E}\rangle\end{aligned}$$

Similar treatment yields

$$\langle \mathrm{B_1}|L_zS_0|\mathrm{B_1}\rangle = -\tfrac{1}{2}\langle \mathrm{E}\|L\|\mathrm{E}\rangle\langle \mathrm{E}\|S\|\mathrm{E}\rangle$$

$$\langle \mathrm{A_2}|L_zS_0|\mathrm{A_2}\rangle = \tfrac{1}{2}\langle \mathrm{E}\|L\|\mathrm{E}\rangle\langle \mathrm{E}\|S\|\mathrm{E}\rangle$$

$$\langle \mathrm{B_2}|L_zS_0|\mathrm{B_2}\rangle = -\tfrac{1}{2}\langle \mathrm{E}\|L\|\mathrm{E}\rangle\langle \mathrm{E}\|S\|\mathrm{E}\rangle$$

In these expressions the reduced matrix elements contain the magnitude of the spin–orbit coupling in the complex. For $[\mathrm{Cu(NN)_2}]^+$ species this is expected to be less than 10^3 cm^{-1}.

Registry No. $[\mathrm{Cu(bpy)_2}]\mathrm{ClO_4}$, 39210-78-1; $[\mathrm{Cu(dmb)_2}]\mathrm{ClO_4}$, 121269-32-7; $[\mathrm{Cu(phen)_2}]\mathrm{ClO_4}$, 23624-03-5; $[\mathrm{Cu(bcn)_2}]\mathrm{ClO_4}$, 23523-22-0; $[\mathrm{Cu(2,9\text{-}Me_2\text{-}phen)_2}]\mathrm{ClO_4}$, 41574-54-3; poly(methyl methacrylate), 9011-14-7.

---

[20] Mulliken, R. S.; Person, W. B. *Molecular Complexes. A Lecture Note and Reprint Volume*; Wiley-Interscience: New York, 1969.

[21] Parker, W. L.; Crosby, G. A., to be published.

[22] Silver, B. L. *Irreducible Tensor Methods*; Academic Press: New York, 1976.

[23] Griffith, J. S. *The Irreducible Tensor Method and Its Application to Molecular Symmetry Groups*; Prentice Hall: Englewood Cliffs, NJ, 1962.